HESS J1857+026 analysis

Page under construction.

This page summarize the main points of the analysis I did on HESS J1857+026 using 2 sample of data.

The first analysis used 31 months of data collected from August 4, 2008, until March 2011. Only gamma-rays in the Diffuse class events were selected and we excluded those coming from a zenith angle larger than 100°.We have used the P6_V11_Diffuse instrument response functions (IRFs). We included in the model all the sources of the 18 month catalog and assiociated diffuse files.

The second analysis used the same amount of data. Only gamma-rays in the source class events were selected and we excluded those coming from a zenith angle larger than 100°. We have used the P7_V6_SOURCE IRFs. We included in the model all the sources of the 2FGL catalog and assiociated diffuse files.

The Region of Interest.

HESS J1857+026 is in the same region than the SNR W44 which is the brightest source of the region.

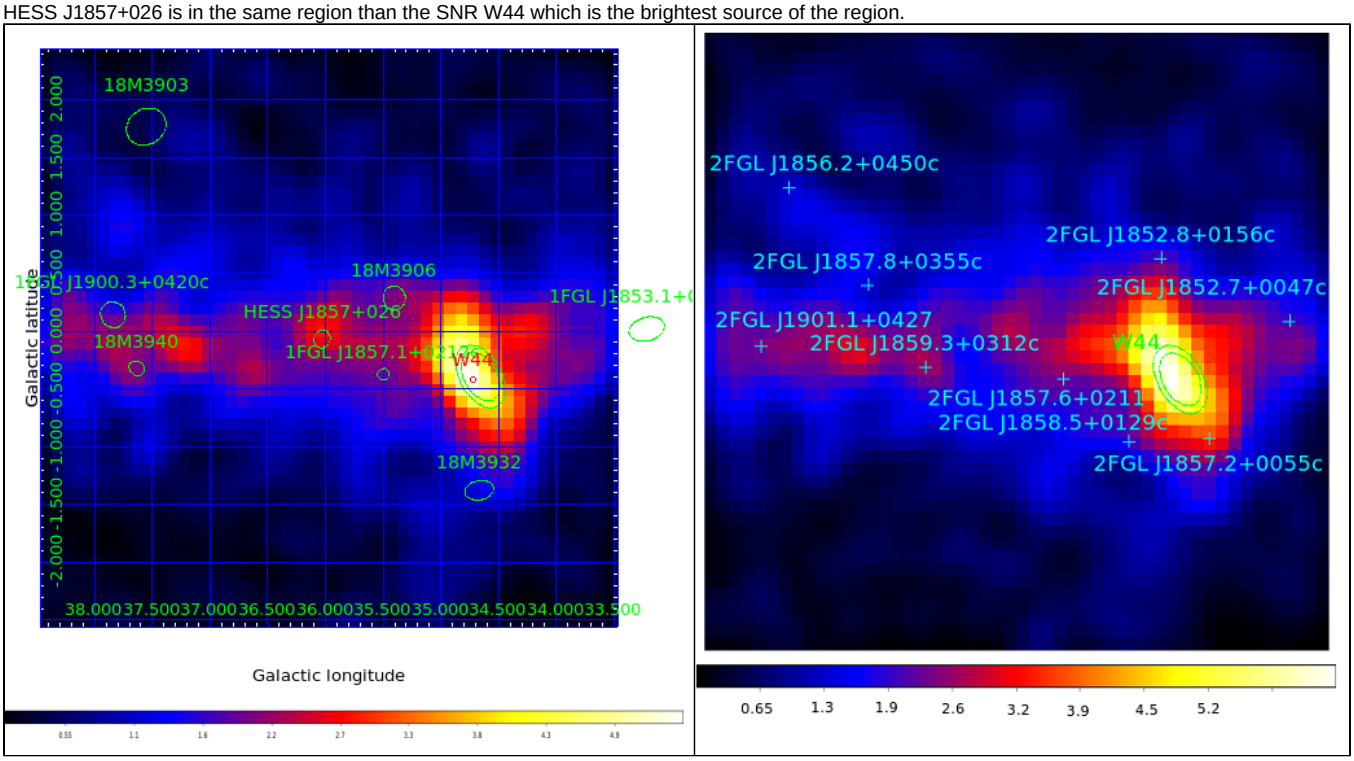

Fig 1. Counts map of the region above 6 GeV. Left Pass 6 analysis with 18 months catalog sources in green. Right : Same picture corresponding to the Pass 7 analysis with 2FGL sources represented in blue.

W44

The shape of W44 was fitted by an Elliptical Ring (ref. 1) and it spectra by a broken power law.

We saw an excess close to W44 and tried to refit the source to take into account this excess.

We refitted again the spectra of W44 by a Log-Parabola and studied the shape of W44.

The main point is that the results are consistent with previous work and with 2FGL cat.

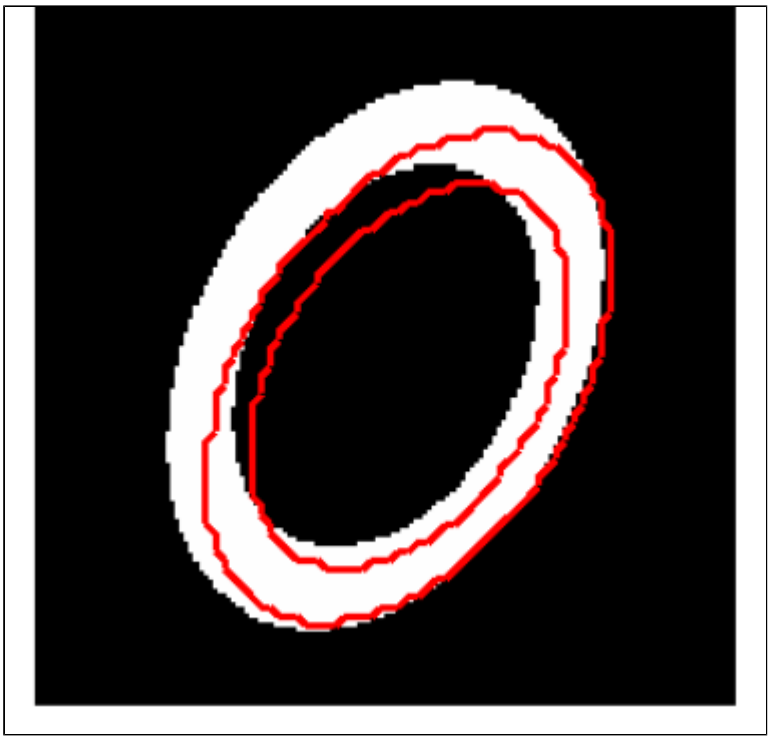

Fig. 2. Comparison between the result of ref. 1 (red contours) and our results using pass 6 (white ring) . There is no error taken into account in this templates. Figure to be updated with Pass 7

Model	RA(°)	DEC(°)	Semi Major Axis (°)	Semi Minor Axis (°)	Pos.Ang. (°)
T. Tanaka (1)||||||||||||||||	283,990	1,355	0,300	0,190	327,000
Pass 6	284.015(+/- 0.004)	1.392(+/- 0.005)	0.335(+0.117 -0.086)	0.207 (+0.023 -0.021)	330+/- 25
Pass 7	284.000(+/- 0.006)	1.374(+/- 0.006)	0.332(+0.109/- 0.079)	0.205 (+0.021/- 0.017)	327 +/-22

Table 1. Parameters obtained by fiting the shape of W44. The main point is that all of these values are consistent with the work of Tanaka et al. 2010.

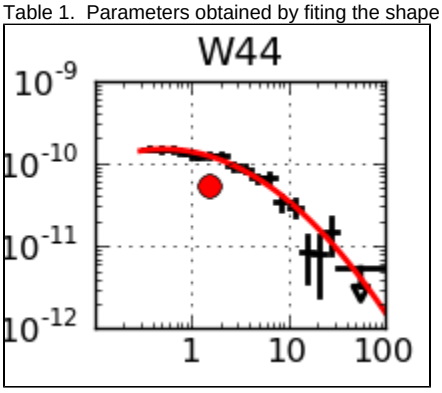

Fig. 3 SED of W44 given by pointlike.

Adding a new source to Pass 7 Analysis

section under construction

Using 2FGL sources, Pass 7 IRFS and associated diffuses, we found a low energy excess quickly decreasing with energy.

To prevent contamination from this source on HESS J1857 we analysed it. The best fit we obtained is a point source located at

RA=283.58 DEC=2.98

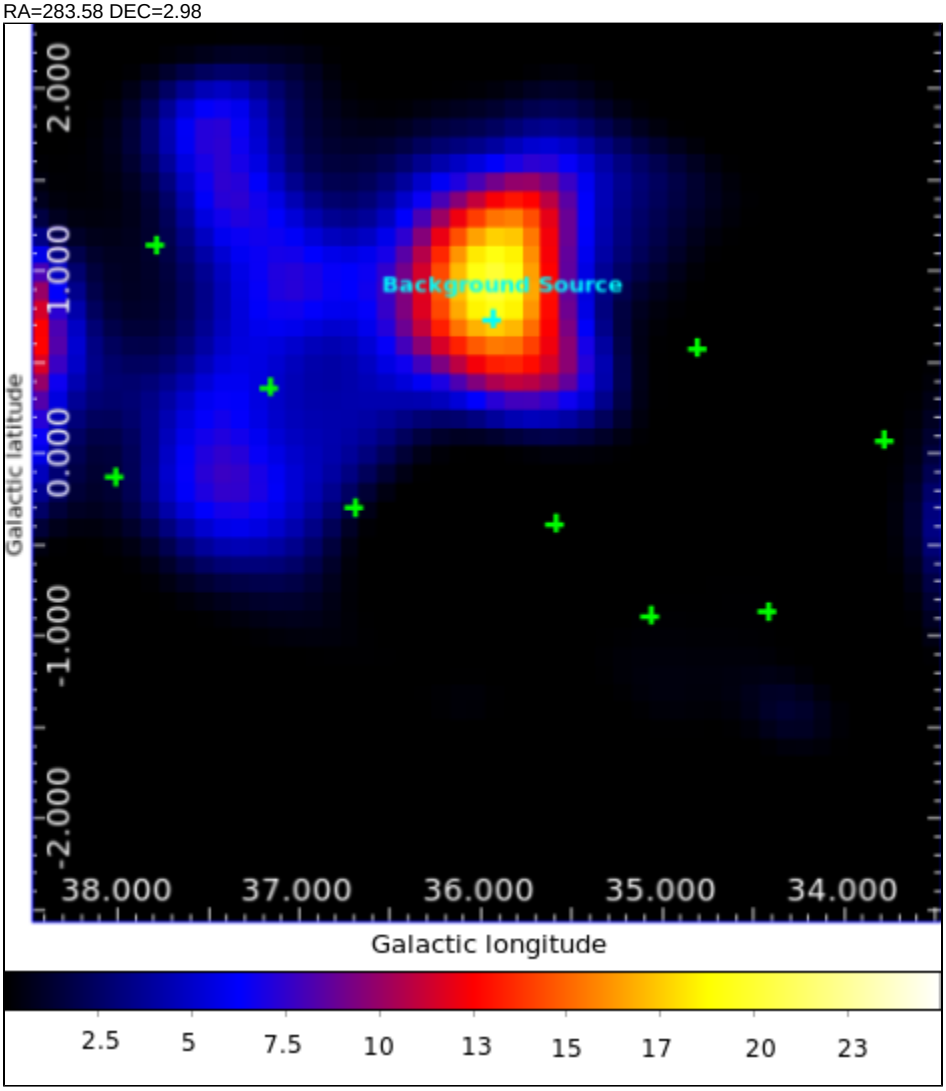

Fig. 4. Residual TS map between 100MeV and 1.3GeV using pointlike. Green crosses represents 2FGL sources

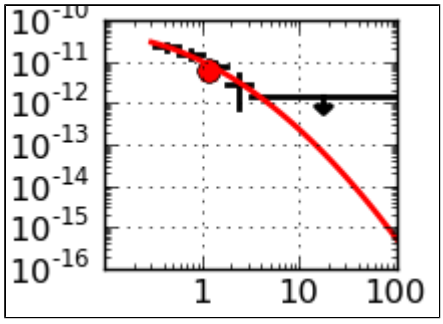

Fig. 5. SED of the source using pointlike.

The best fit using gtlike provided the following parameters and statistical errors alpha = 3.5 +/- 0.2, beta = 0.6 +/- 0.1, Eb ? 1.2 GeV, and N_0 = (3.1 +/- 0.5) X 10^{-12} photons/MeV/cm^2/s.

Search for pulsed emission

A.LYNE, B. STAPPERS and C.ESPINOZA kindly provided us timing solution of PSR J1856+0245 which powers HESS J1857+026.

Marie-Helene searched for pulsation concidering 43 pulsars in 3° around the HESS position but found no pulsed emission from PSR J1856+0245. H-Test <<2.

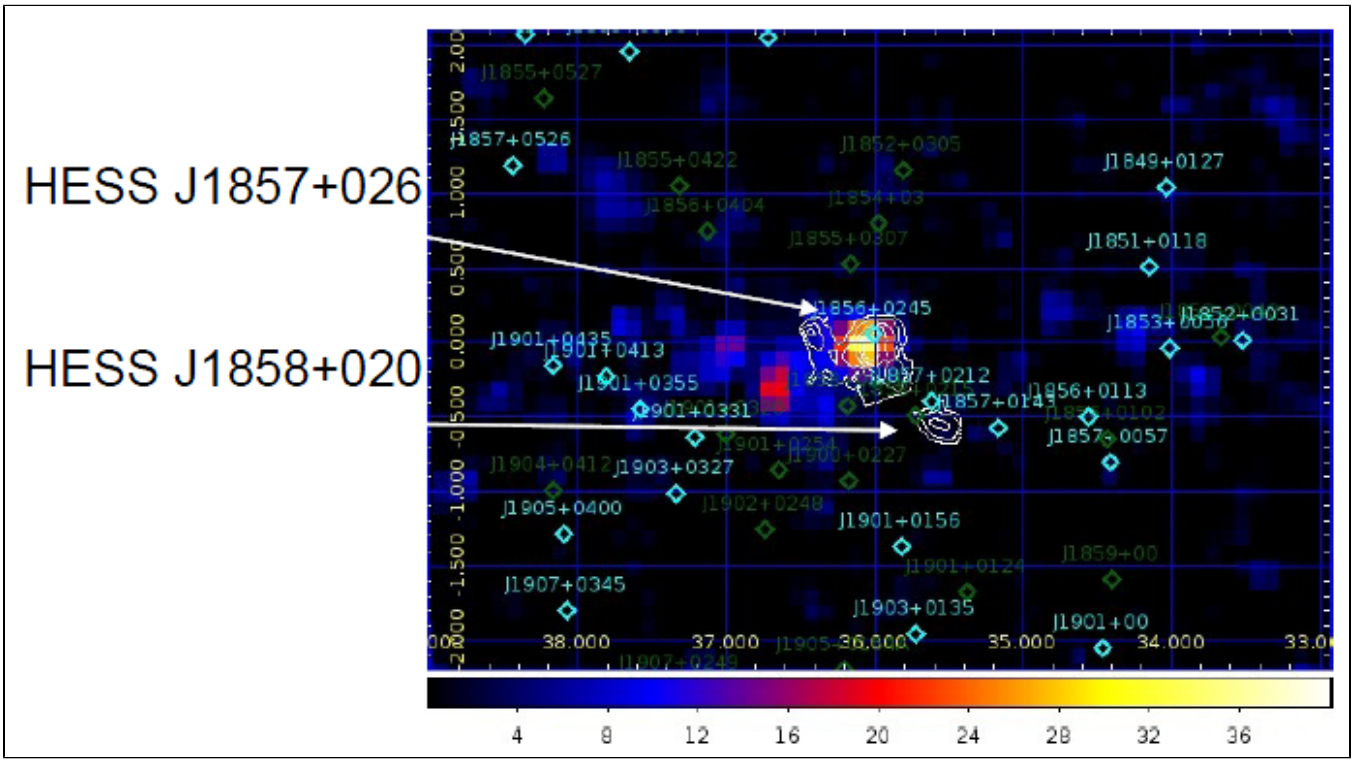

Fig.6 TS map above 10GeV using Pass6_V11. HESS J1857 is not included in the model. white contours are those obtained using HESS data. Cyan : Pulsars monitored by radio-telescopes. Green : Other pulsars (from the ATNF database)

Only one good candidate was found : PSR J1856+0113 located in W44 :

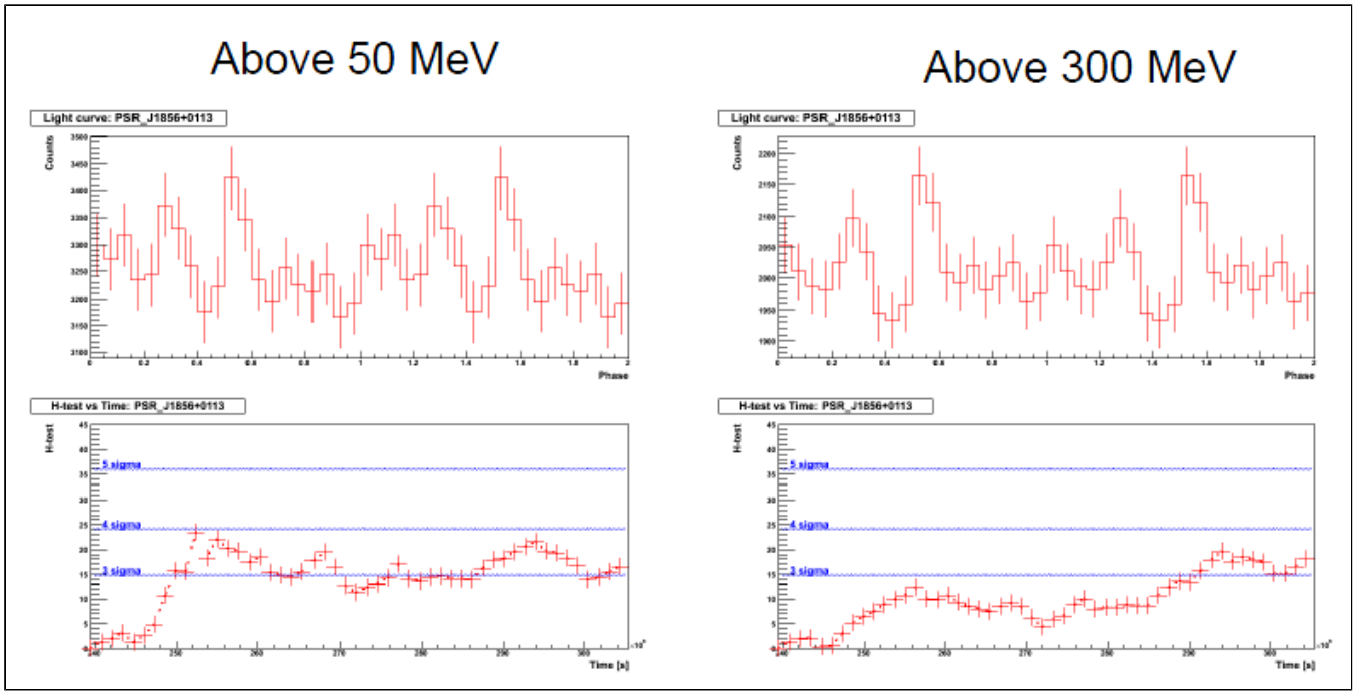

Fig. 7. Light curves and H-Test obtained looking at PSR J1856+0113 above 50 MeV and 300MeV.

HESS 1857+026 Morphology above 10GeV

To avoid any contamination from other sources or diffuse emission from the Galactic plane we tested for extension above 10 GeV. All the sources previously announced were taken into account (18 months -> Pass 6, 2FGL +1 ->Pass 7).

Hypothesis	Point	Gaussian	Disk
TS	33.38	41.35	42.21
?TS	-	7.97	8.83

Table 2. TS and Loglike found above 10GeV for a point source, a gaussian and a Disk. Pass 6 analysis.

Hypothesis	Point	Gaussian	Disk
TS	14.6	20.1	18.3
?TS	-	5.5	3.7

Table 3. TS and Loglike found above 10GeV for a point source, a gaussian and a Disk. Pass 7 analysis.

Analysis	RA (°)	DEC (°)
HESS	284.3	2.68
Pass 6	284.28	2.74
Pass 7	284.31	2.76

Table 4. Fited positions.

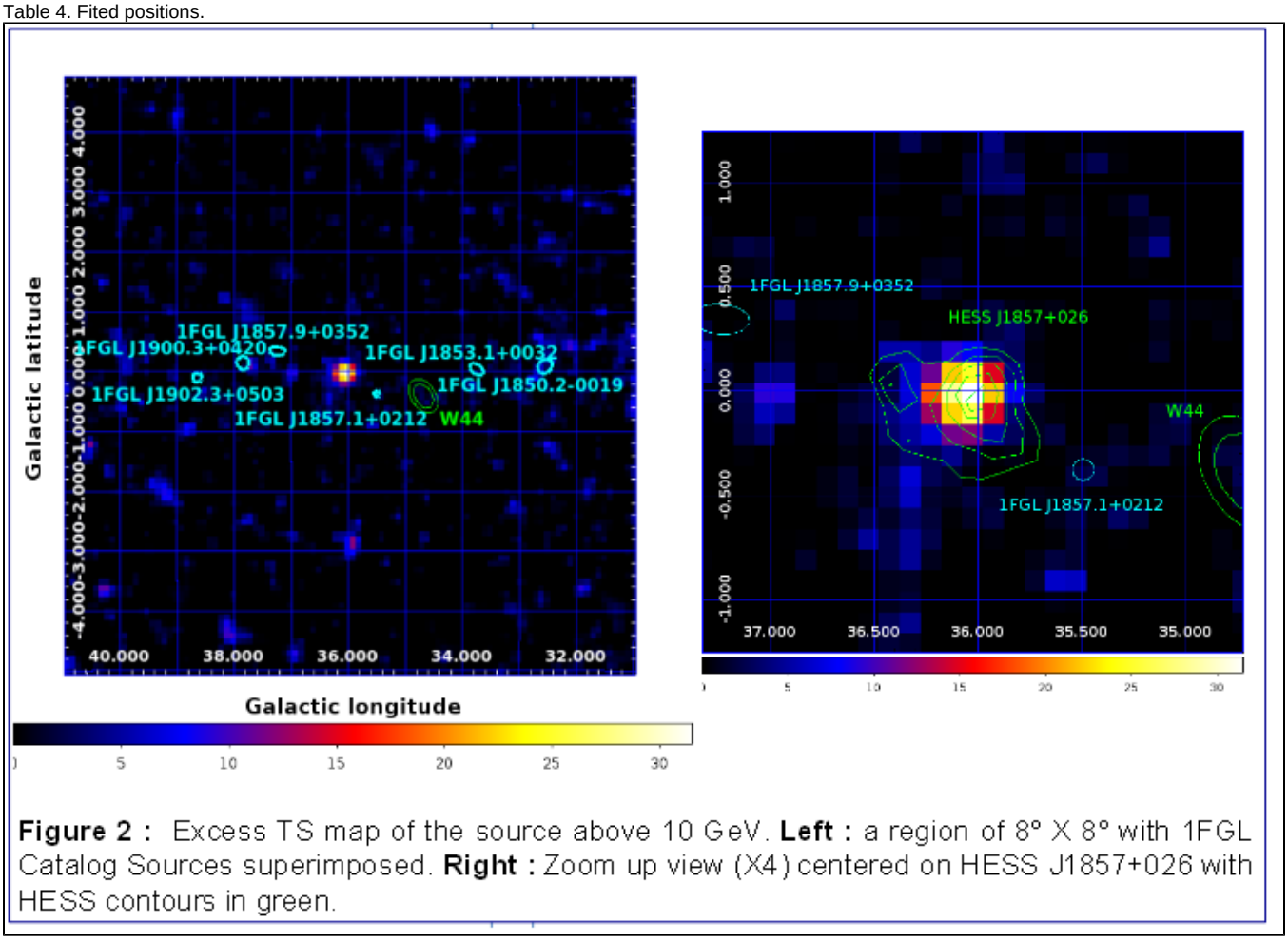

Figure 2 : Excess TS map of the source above 10 GeV. **Left :** a region of 8° X 8° with 1FGL Catalog Sources superimposed. **Right :** Zoom up view (X4) centered on HESS J1857+026 with HESS contours in green.

Fig. 8. Residual TSMap in which HESS J1857 is not fitted. Pass 6 analysis. + HESS contours

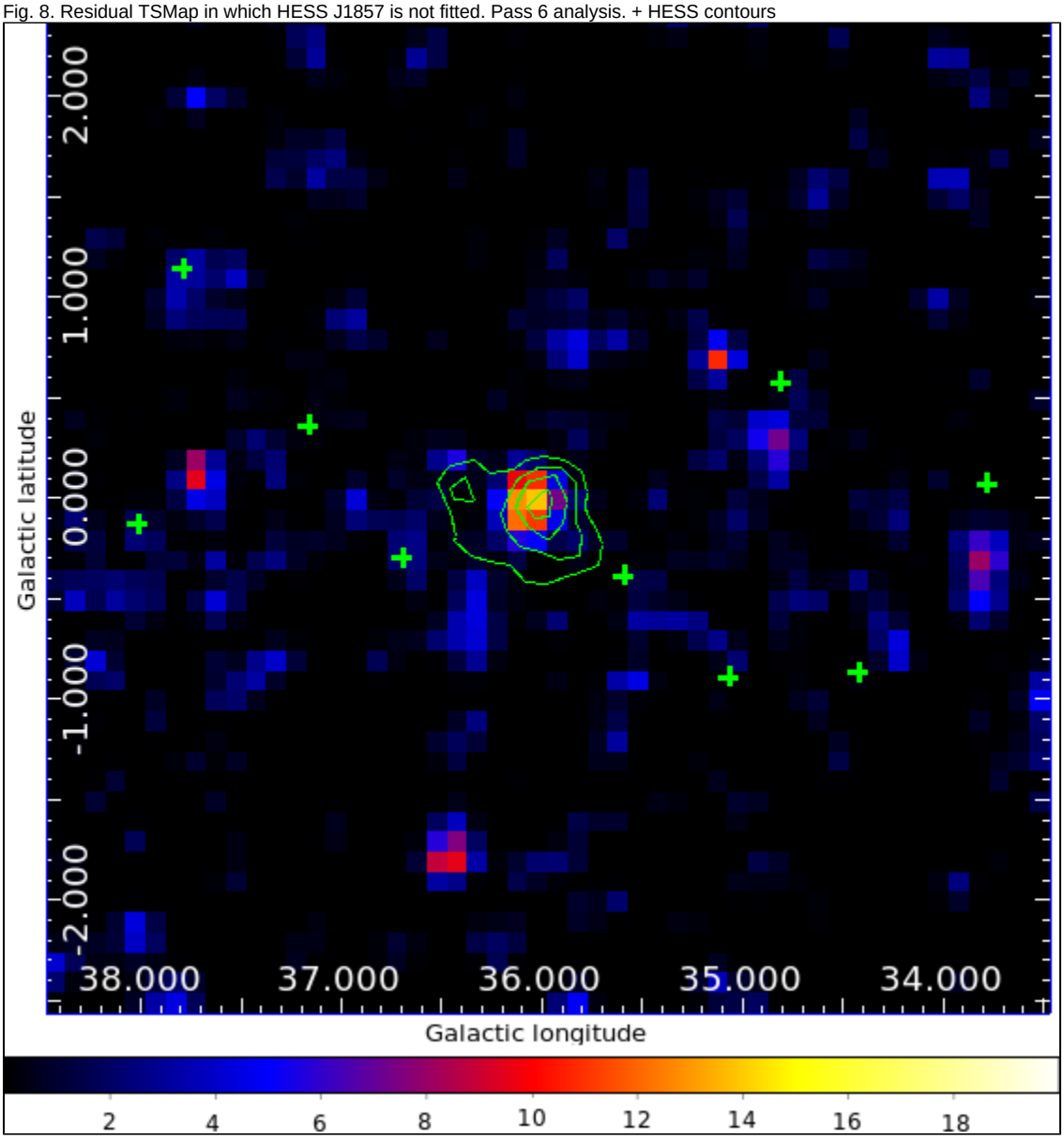

Fig 9. Residual TSMap in which HESS J1857 is not fitted. Pass 6 analysis. + HESS contours. Green crosses represents 2FGL sources.

Spectral analysis

We fitted the source using pointlike above 300GeV to prevent contamination at low energy.

Here are the summary of the Pass 6 analysis :

The best fit obtained using pointlike gave the following parameters :

Int. Flux (>100MeV) 10^{-9} ph/cm^2/s	-1 X Index	Lower Limit (MeV) Frozen	Upperlimit (GeV) Frozen	TS
8.19+/-1.71(stat)	1.65+/-0.06 (stat)	100	100	49.73

Table. 5. Parameters of the best fit obtained using pointlike on Pass6.

Those gave the following SED :

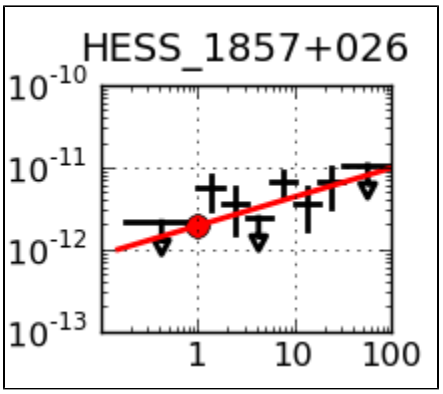

Fig. 10 SED obtained with pointlike using Pass

Using Pass 7 with 31 months of data the source is fitted by a hard power law. The parameters of the best fit are those of the next table :

IRFS	Int. Flux (>100MeV) 10^{-9} ph/cm^2/s	-1 X Index	Lower limit (MeV) Frozen	Upper limit (GeV) Frozen	TS	gal
Pass 7	5.67+/-0.65+/-3.2	1.65+/-0.27+/-0.31	100	100	28.1	1.09

Table. 6. Parameters of the best fit obtained using gtlike.

With more data

To compare our spectral points to those obtained with MAGIC (talk at the ICRC Klepser et al., Mapping the extended TeV source HESS J1857+026 down to
Fermi-LAT energies with the MAGIC telescopes) we reanalyzed the source to 300 MeV using more data (36 months instead of 31). Here are the results obtained :

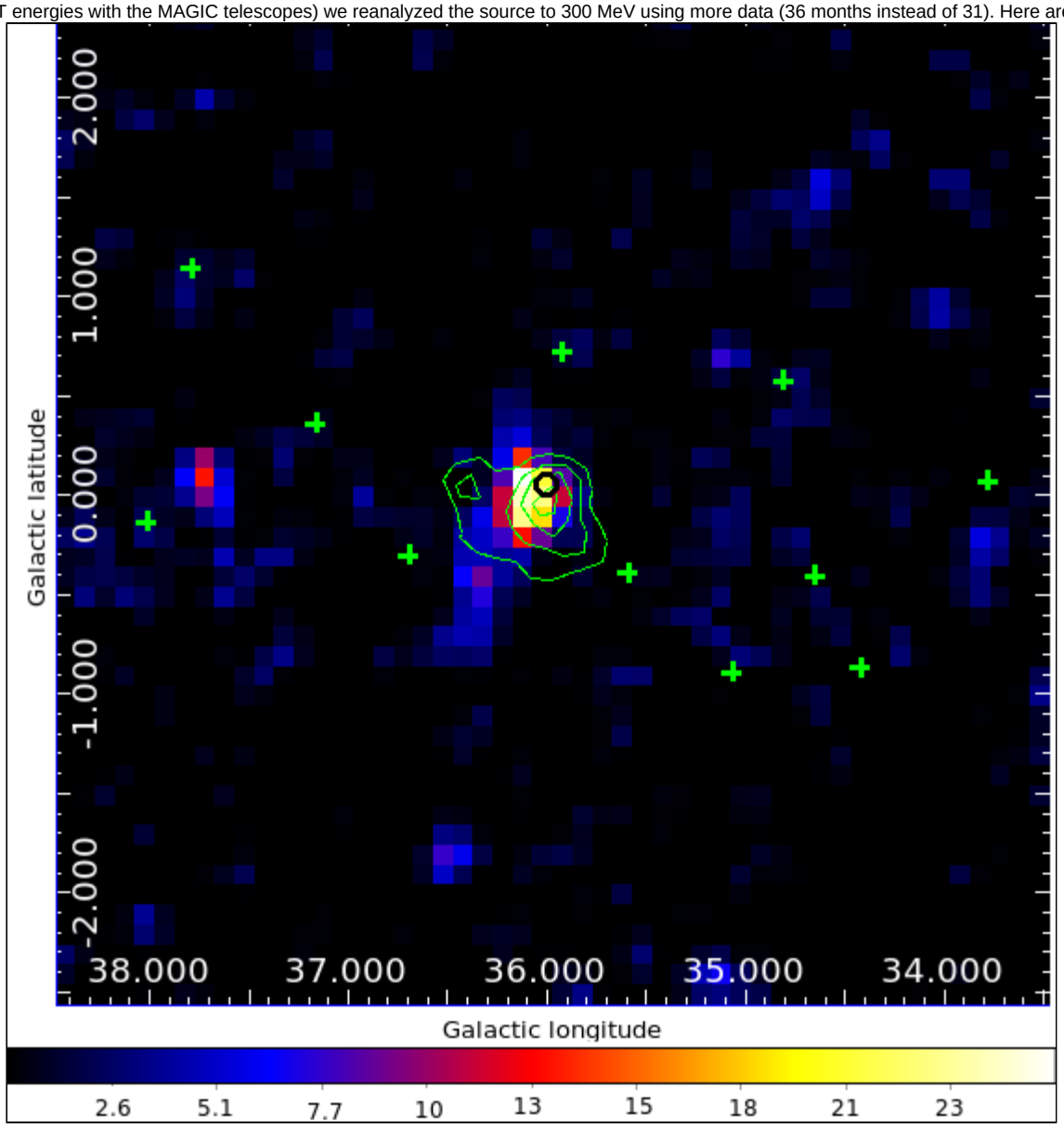

Fig. 11 Residual TS map obtained between 10GeV and 300GeV. Here HESS J1857 is not included in the model. The green contours are those obtained using HESS data (Aharonian et al.,2008).

The position of the Fermi excess is consistent with those of HESS. The black circle represents the position of PSR J1856+0245.

IRF	Int Flux(100MeV-100GeV) MeV/cm^2/s	Index	Lower limit (MeV) (frozen)	Upper limit (GeV) (frozen)	TS	gal
P7SOURCE_V6	(5.79 ± 0:75 ± 3.11)X10^{-9}	1.52 ± 0.16 ± 0.55	100	100	38.7	1.09

Table 7: Best fit parameters for 36 month of data fitting between 300MeV and 300GeV.

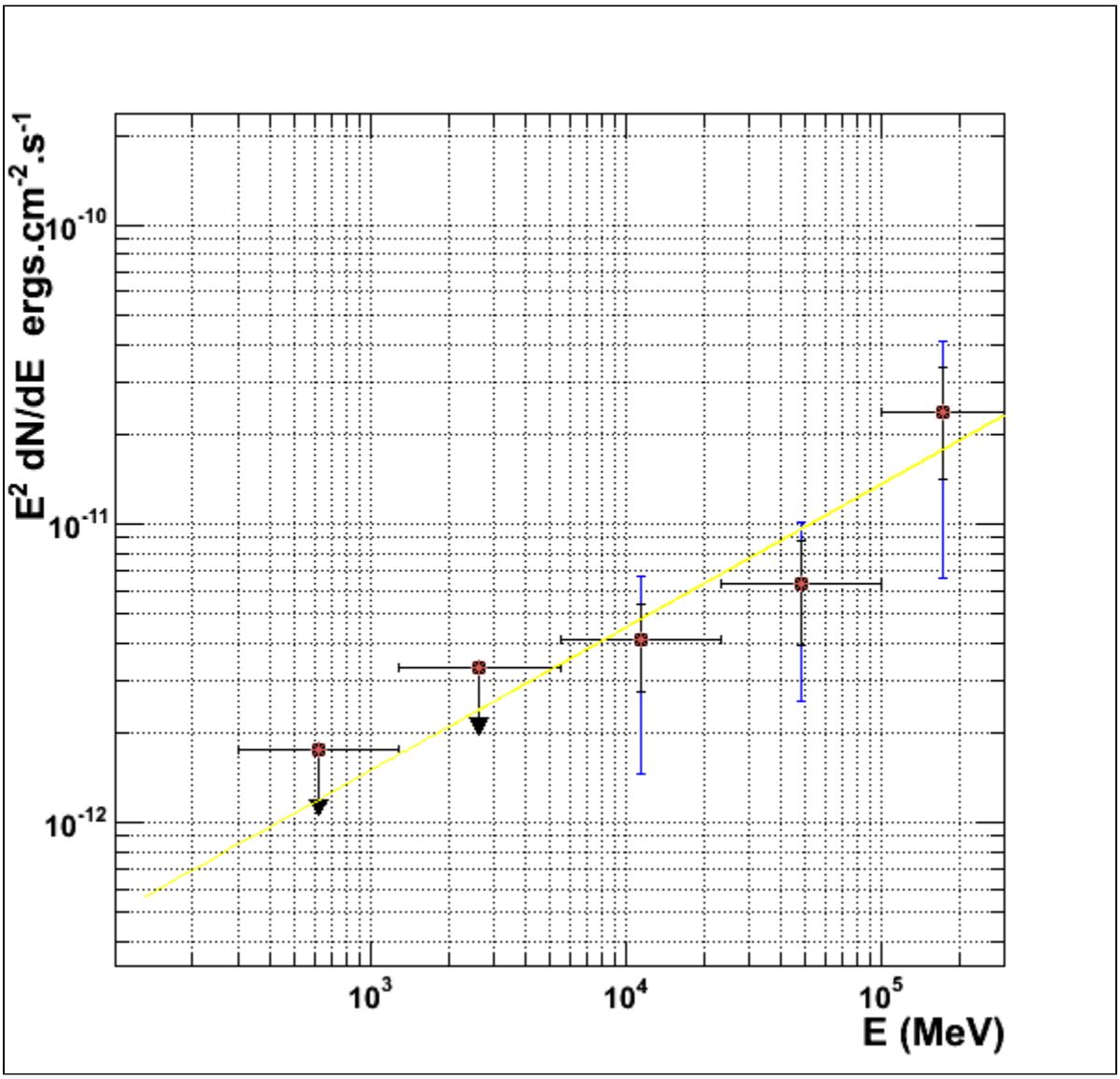

Fig. 12 : SED obtained using gtlike above 300 MeV. The best fit is show in yellow. Statistic and systematics error bars are respectively the black and blue lines.

We added one source of systematics using a template consistent with those of HESS data (Aharonian et al.,2008). The SED thus obtained is consistent with the one shown by Klepser et al. at the ICRC.

Assuming a distance of 9kpc we derived the luminosity of the PWN to compute its gamma efficiency. We obtained :

L (PWN) = 2.49 X 10^35 ergs/s.

Using the pulsar Edot =4.6 X 10^36 we computed an efficiency of 5.4%. To compare to the 3.1% obtained using HESS data.

This efficiency is consistent with what is expected from Ackerman et al. 2011 (the order of magnitude of the percent) as is shown in the following picture :

Fig. 13 ?-ray Luminosity of the Pulsar Wind Nebulae as a function of the spin-down luminosity of the associated pulsar. All the pulsar wind nebulae detected by Fermi are associated with young and energetic pulsars. Pulsar wind nebulae detected by Fermi are marked with red stars. Blue squares represent pulsars for which GeV ?-ray emission seems to come from the neutron star magnetosphere, and not from the nebula.

Using our model we derived and upper limit on the DC emission of the pulsar :

F(100MeV-100GeV)< 1.04e-8 ph/cm2/s leading to a limit on the gamma-ray luminosity of 7.47e34 erg/s.

Supporting X-Ray measurement

To obtain a precise flux for any potential X-ray PWN associated with PSR J1856+0245, we analyzed a 39-ks Chandra ACISI observation (Obs. ID 12557) using CIAO version 4.3.1 with CALDB 4.4.3. PSR J1856+0245 is clearly detected as a point source, but there was no immediate evidence for extended emission surrounding this position. Given that the size of the potential X-ray PWN is not known, we investigated two extraction regions to see whether they produce a statistically significant excess of counts compared with the background. These two extraction regions were in the form of annuli extending from 2"- 7" and 2"-15" respectively from the position of the pulsar. The background regions were chosen from several other source free regions in the vicinity of the pulsar. For the 2"- 7" extraction region we find an upper limit on the unabsorbed flux of 2X10^14 erg/s/cm2 (1-10 keV, 3? confidence), corresponding to a luminosity of 2X10^32 erg/s. The background-subtracted counts in this region show a 1.7? excess from zero. For the 2"-15" extraction region we find an upper limit on the unabsorbed flux of 5 X 10^14 erg/s/cm2 (1 - 10 keV, 3? confidence), corresponding to a luminosity of 5X10^32 erg/s. The counts in this region show a 2? excess from zero counts. Given the marginal significance of the count excesses in both cases we cannot convincingly claim the detection of a weak X-ray PWN. These luminosity limits are derived from the 3? upper bound on the net count rate and assume a typical powerlaw spectrum of index 1.5 for the PWN, a distance of 9 kpc, and a column density NH = 4X10^22 cm^2. An in-depth analysis of the X-ray properties of PSR J1856+0245 will be presented elsewhere.

Discussion

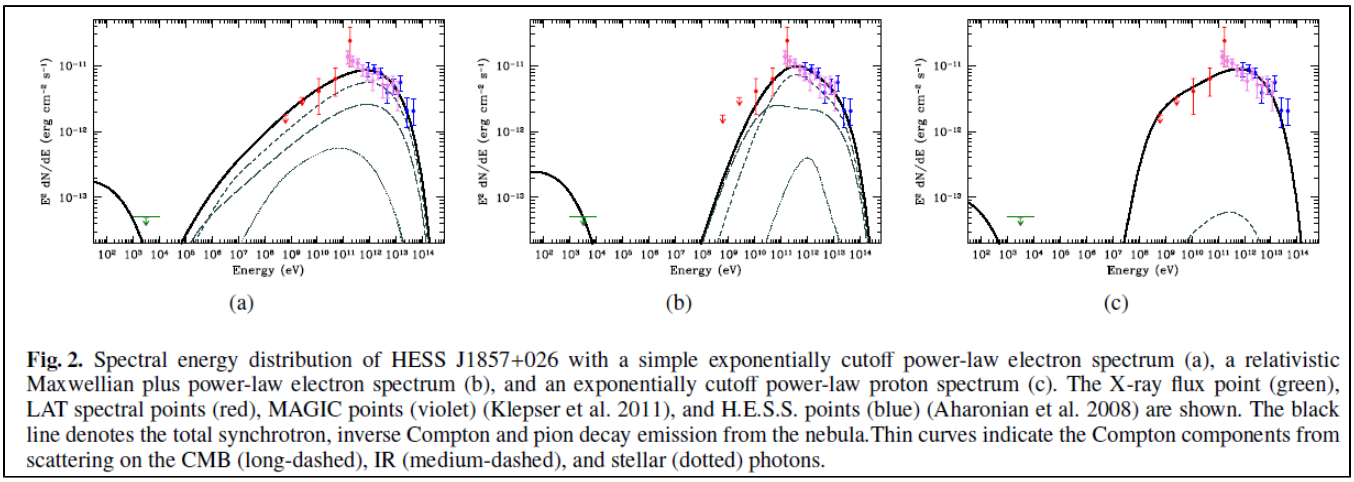

Fig. 2. Spectral energy distribution of HESS J1857+026 with a simple exponentially cutoff power-law electron spectrum (a), a relativistic Maxwellian plus power-law electron spectrum (b), and an exponentially cutoff power-law proton spectrum (c). The X-ray flux point (green), LAT spectral points (red), MAGIC points (violet) (Klepser et al. 2011), and H.E.S.S. points (blue) (Aharonian et al. 2008) are shown. The black line denotes the total synchrotron, inverse Compton and pion decay emission from the nebula.Thin curves indicate the Compton components from scattering on the CMB (long-dashed), IR (medium-dashed), and stellar (dotted) photons.

Fig. 13 SED modeling

To investigate the global properties of the PWN, we apply a one zone time dependent SED model, as described in Grondin et al. (2011b) and Abdo et al. (2010a). This model computes SEDs from evolving electron populations over the lifetime of the pulsar in a series of time steps. During the free-expansion phase of the PWN (assumed to be ~ 104 years) we adopt an expansion of R / t, following which the radius evolves as R / t^0.3, appropriate for a PWN expanding in pressure equilibrium with a Sedov phase SNR. Over the pulsar lifetime the magnetic field evolves as B / t^1.5, following ~500 years of constancy. We fix the pulsar braking index to the canonical value of 3.

We assume the existence of three primary photon fields (CMBR, far IR (dust), and starlight) and use the interstellar radiation mapcube within the GALPROP suite (Porter et al. 2005) to estimate the photon fields at the Galactic radius of PSR J1856+0245. A distance of 9 kpc in the direction of the pulsar corresponds to a Galactic radius of 5.4 kpc. At this radius, the peak of the SED of dust IR photons corresponds to a black body temperature of T ~ 32 K with a density of ~ 1.1 eV cm^3, while the SED of stellar photons peaks at T ~ 2500 K with a density of ~ 1.2 eV cm^3.

Spectral measurements consist of LAT, MAGIC (Klepser et al. 2011) and H.E.S.S. (Aharonian et al. 2008) data points, as well as the 2" - 15" X-ray upper limit described above.

A simple exponentially cutoff power-law injection of electrons, evolved properly over the pulsar lifetime, often provides an adequate match to PWNe SEDS. For this injectin spectrum we fit four variables: final magnetic field Bf = 0.8 +/ - 0.4 ?G, electron high energy cuto Ecut = 66 -+/ 16 TeV, electron powerlaw index p = 2.25 +/- 0.03, and initial pulsar spin period P0 = 9.9 +/- 6.1 ms, which gives an age of 20 kyr. This model yields a 2=do f = 23/9=21 and poorly matches the low energy MAGIC points, as shown in Figure 2 (Left).

Another option to fit the multi-wavelength data is to adopt the relativistic Maxwellian plus power-law tail electron spectrum proposed by Spitkovsky (2008). We implement this spectrum as described in Grondin et al. (2011b). The best fit, presented in Fig. 2 (Middle), is obtained with kT = 0.96 +/- 0.17 TeV corresponding to an upstream gamma-factor of 3.7 X 10^6, a magnetic field of Bf = 1.0 +/- 0.9 ?G, a cutoff at Ecut = 92 +/- 26 TeV and a power-law index of p = 2.45 +/- 0.12, consistent with the value of ~ 2.5 proposed by Spitkovsky (2008). The braking index of n = 3 and initial spin period of P0 = 48 +/- 4 ms give an age of 13 kyr. The relativistic Maxwellian plus power law model better matches the multi-wavelength data, with a 2=do f = 13.6=20. A hadronic scenario is also possible, with -rays arising from proton-proton interactions and subsequent pion decay. For this model, corresponding to Fig. 2 (Right), we fix the ambient gas density at 50 cm^3 and age at 20 kyr. We find a best fit of

2=do f = 24/7=21 with a magnetic field of Bf = 10 +/- 20 ?G,proton cuto at Epcut = 73 +/- 27 TeV, a proton power-law index of

p = 1.83 +/- 0.03, and an energy content in protons of 6.9 +/- 0.6 X 10^49 erg.

The MAGIC and H.E.S.S. data combine to form a powerlaw spectra of index ~ 2.3 over nearly three decades in energy. This VHE data, combined with the limits imposed by the steep LAT data, is diffcult to match with a simple power-law injection of electrons (or protons), and we find a significantly better fit with a relativistic Maxwellian plus power-law spectrum. Yet the exceedingly low magnetic field of the leptonic fits, due to the stringent X-ray upper limit, call into question these models. Such a low magnetic field implies that if PWN leptons are indeed responsible for the
-ray flux, they must be dominated by relic electrons which have escaped the PWN core into very
weakly magnetized surroundings. The hadronic scenario relaxes this constraint, though the energy requirements are quite high even for a dense ambient medium, and a very hard power-law index is required. At present the true nature of HESS J1857+026 remains a mystery, though the new LAT data and X-ray upper limit hint that this source is far from the typical TeV PWN.

In the paper

I'm now writting the draft of an A&A letter with M.-H. Grondin, M. Lemoine-Goumard, A.Van Etten, B. Stappers, A. Lyne, C. Espinoza.

The first part is an introduction of the source.

The second part summarize the data I used.

The third part (Fermi data analysis) is divided in 2

1. Search for pulsation. -> No pulsed emission
2. Spatial and spectral analysis

- Spatial
- Spectral

The fourth part summarize the X-Ray observations

The discussion begins with the SED modeling and present the gamma-ray luminosity and efficiency.

I would like to show 3 figures which are th Fig. 4, 14 and 16(comming soon).

The draft is coming soon.

Bibliography :

(1) Abdo et al., Science,327, 1103-1106, 2010

(2) Hessels et al., ApJ, 682, L41-L44, 2008
(3) Aharonian et al., A&A, 477, 353-363, 2008

(4) Cordes, J. M., & Lazio, T. J. W. 2002, preprint (astro-ph/0207156)
(5) Vincent, M., Thesis : “Nebuleuse de pulsars : sondage profond de la Galaxie au TeV et études multi-longueur d'onde”.

(6) Sugizaki et al., ApJ Supplement Series, 134, 77-102, 2001

(7) Ackermann et al., ApJ, 726, 35-102, 2011